

DESIGN CONSIDERATIONS OF THE FINAL TURNAROUND REGIONS FOR THE CLIC DRIVE BEAM

R. Apsimon[#], J. Esberg, A. Latina, D. Schulte, J. Uythoven, CERN, Geneva, Switzerland

Abstract

The optics design of the final turnaround regions for the CLIC drive beam is presented. This includes the extraction region, the turnaround loop and the phase feed forward chicane for correcting errors on the bunch phase. The design specifications of the kicker and septum magnets are provided. Tracking simulations and detailed studies of coherent and incoherent synchrotron radiation have been used to optimise the optics in the turnaround region in order to minimise transverse and longitudinal emittance growth.

INTRODUCTION

The Compact Linear Collider (CLIC) is a proposed electron-positron collider with a centre of mass energy of 3 TeV. The CLIC design uses a novel two-beam acceleration scheme. The main linac consists of normal-conducting RF cavities; the RF power is provided by a 2.38 GeV drive beam [1]. The drive beam is a ~ 100 A beam consisting of 48 bunch pulses. Each bunch pulse passes through one of the decelerating structures, known as power extraction and transfer systems (PETS). The energy lost from the drive beam is used to accelerate the main beam from 9 GeV to 3 TeV with an accelerating gradient of ~ 100 MV/m. In order to accelerate the main beam, the RF power must travel in the same direction; therefore, so must the drive beam. To do this, turnaround loops (TALs) are required to redirect the drive beam so that it enters the PETS from the correct direction. Figure 1 is a sketch of the main linac and PETS, showing that the main beam and drive beam travel in opposite directions before the TALs [1].

DESIGN CONSIDERATIONS

The luminosity loss at the interaction point is quadratically dependent on amplitude and phase jitter of the accelerating RF in the main linac [2]. The RF phase jitter is directly related to the phase jitter between main and drive beams. The amplitude jitter is related to charge and form factor variations of the drive beam. The tolerances on the accelerating RF are $\sim 0.2\%$ for amplitude jitter and $\sim 0.3^\circ$ at 12 GHz for the phase jitter [1,3].

To relax the tolerances on incoming phase jitter, a phase feed forward system is foreseen for the TALs [3]. A

vertical 4-bend chicane would be situated downstream of the TAL and kickers would be used to alter the amplitude of the chicane and therefore the path length. A similar chicane would also be situated upstream of the TAL in order to measure the phase jitter between main and drive beams as well as to alter the bunch length through the TAL.

The long transfer lines (LTLs) which transport the drive beam to the PETS consists of 109.6 m FODO cells with a phase advance of 45° . The beam is extracted from the LTL into the TAL by one kicker magnet followed by a thin and thick septum. The design parameters for the extraction kicker and septa are provided in Tables 1 and 2.

Table 1: Extraction Kicker Parameters

Parameter	Value
Kicker length	5 m
Kick angle	2.1 mrad
Rise/fall time	5 μ s
Flat-top duration	300 ns
V-kicker aperture	20 cm (full)
Kicker type	Wound core / ferrite loaded

Table 2: Extraction Septa Parameters

Parameter	Thin septum	Thick septum
Length	0.9 m	0.7 m
Deflection angle	18 mrad	65 mrad
Dipole field	0.2 T	1.0 T
Septum thickness	1 cm	2.5 cm
Vertical aperture	5 cm	5 cm

After the extraction cell a dispersion suppression region is used to remove the dispersion from the extraction and to correct the angle of the beam so that it travels parallel to the LTL. Figure 2 shows the horizontal layout of the TAL region. The arc region consists of 5 arc cells and a straight section. The negative arc cell and the straight section are used to correct the horizontal offset after the TAL; the four positive arcs form the main arc section.

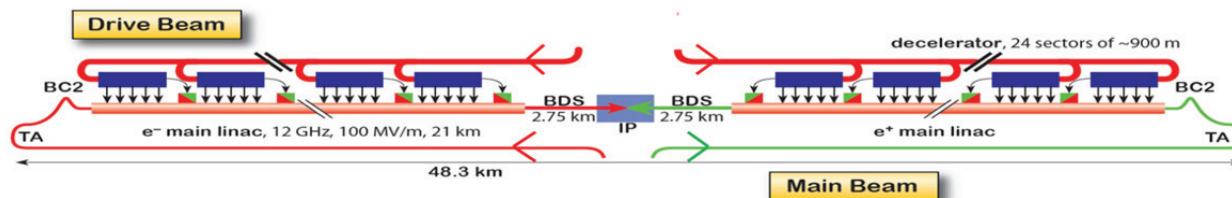


Figure 1: Sketch of the main linac and PETS.

[#]robert.apsimon@cern.ch

Content from this work may be used under the terms of the CC BY 3.0 licence (© 2014). Any distribution of this work must maintain attribution to the author(s), title of the work, publisher, and DOI.

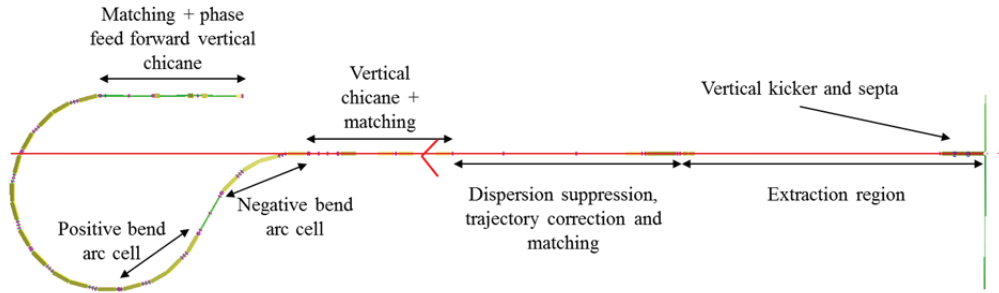


Figure 2: Diagram of the TAL layout.

The TAL region must be globally isochronous ($R_{56}=0$); therefore the arc cells must have a variable R_{56} to correct the contributions from the chicanes and extraction region.

Due to the large energy spread of the bunches ($\sim \pm 1\%$) it is important to limit chromatic aberrations as well as coherent and incoherent synchrotron radiation (CSR and ISR) to minimise emittance growth. Sextupoles are planned to correct the chromatic aberrations. Both CSR and ISR emittance growth is proportional to a scaling factor, $\langle H \rangle$, where H is:

$$H = \gamma D^2 + 2\alpha DD' + \beta D'^2. \quad (1)$$

$\langle H \rangle$ is the mean value of H through all the dipoles in the lattice, α , β and γ are the Twiss parameters and D and D' are the dispersion and its derivative in the horizontal plane.

Two types of arc cell were considered for this design; a three bend achromat (TBA) as proposed in [4] and a modified Chasman-Green (CG) cell [1].

Three Bend Achromat

As all three dipoles deflect in the same direction, this design provides the minimum total deflection to the beam; reducing the emission of synchrotron radiation. The maximum dispersion in this design is 0.59 m, therefore $\langle H \rangle$ is relatively small and little emittance growth due to CSR and ISR is expected.

However, this design requires strong quadrupoles, which introduce large chromatic effects. Strong sextupoles are required for the chromatic terms; which introduces higher order terms; limiting the energy acceptance. There are 8 distinct sets of solutions for the optics, thus finding the globally optimal design is not trivial [4].

Modified Chasman-Green Cell

The normal CG cell is a two bend achromat favoured by high-brightness light sources due to its low equilibrium emittance. This is due to the weak quadrupoles; leading to small chromatic aberrations.

R_{56} is defined as shown in the following equation:

$$R_{56} = \int \frac{D(s)}{\rho(s)} ds \quad (2)$$

Where $\rho(s)$ is the radius of curvature of the dipole magnets. The modified CG cell has a dipole at the centre

of the cell at the point of maximum dispersion. The central dipole bends the beam in the opposite direction to the other dipoles, which allows the R_{56} to be varied.

The relative simplicity of this lattice allows the R_{56} and optics to be varied easily. Weak sextupoles are able to correct the chromatic terms; thus introducing much smaller higher order terms.

The negative deflection in the centre of this cell means that there is a larger total deflection per cell than the TBA. This combined with the large maximum dispersion of 5.26 m means that this cell is more susceptible to ISR and CSR than the TBA design.

Comparison

Due to the low energy of the beam and weak dipole fields, emittance growth due to ISR is expected to be negligible.

The smaller chromatic aberrations for the CG lattice make it the better choice of lattice for the TAL. But the larger value of $\langle H \rangle$ means that CSR is foreseen as a potential issue due to the high bunch charge.

OPTIMISATION METHODS

Two approaches were taken to optimise the lattice for the TAL. Initially, the TAL lattice was locally optimised. Each cell was matched individually and a periodic beam is transported through the arc cells. This approach makes the optics easy to tune for a real machine, but the sextupoles were unable to correct chromatic aberrations.

An alternative approach was taken whereby all the quadrupoles and sextupoles between the two chicanes were globally optimised to minimise all 1st and 2nd order energy derivatives, T_{mn6} and U_{mn66} . This approach proved very effective for minimising nonlinear terms, but the beam is no longer periodic through the main arc (Fig. 3). This is likely to pose significant challenges for operational tuning as does the large $\beta_{\max}/\beta_{\min}$ ratio in both planes.

Figure 4 shows the deviation of the centroid of the beam vs. energy offset. The positional deviation is defined as $\delta r = \sqrt{\delta x^2 + \delta y^2 + \delta z^2}$.

TRACKING SIMULATIONS

Tracking simulations were run in PLACET and MADX-PTC [5,6] and are in good agreement with each other. PLACET was used to simulate the effect of ISR

and CSR; the results of which are shown in Table 3; the suffixes -l and -g represent the locally and globally optimised designs.

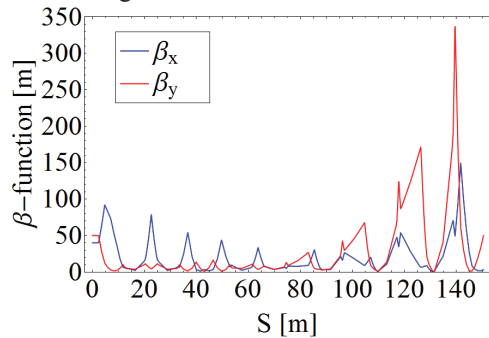


Figure 3: β -functions through the TAL for the globally optimised Chasman-Green optics.

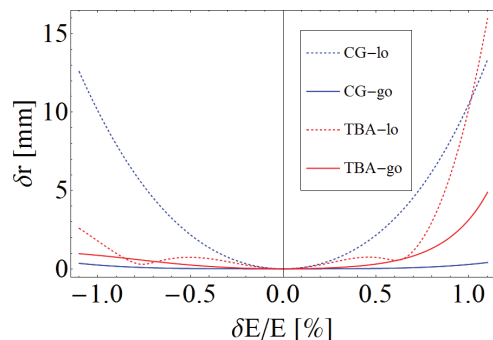


Figure 4: Deviation of beam centroid vs. energy offset.

Table 3: Emittance Growth Studies for Different Lattices

Parameter	TBA-l	TBA-g	CG-l	CG-g
$\langle H \rangle$	0.13	0.12	5.99	0.32
D_{\max} [m]	0.59	0.59	5.26	5.26
Initial ϵ_x [μm]			50	
Initial ϵ_y [μm]			50	
Initial ϵ_z [μm]			3.8	
$\delta\epsilon_x$ no CSR [μm]	169	76	64	3.8
$\delta\epsilon_y$ no CSR [μm]	2	6	1	0.9
$\delta\epsilon_z$ no CSR [μm]	0.05	0	0.6	0
$\delta\epsilon_x$ + CSR [μm]	156	61	246	76
$\delta\epsilon_y$ + CSR [μm]	2.1	5.9	1.3	1.0
$\delta\epsilon_z$ + CSR [μm]	0.5	0.5	1.2	0.6

For both the TBA and CG arc cells, the tracking simulations show a significant reduction in horizontal emittance growth due to the global optimisation. Due to the small $\langle H \rangle$ in the TBA lattice, CSR appears to reduce emittance growth; which is not yet understood. By contrast, the CG lattice is very sensitive to CSR emittance growth; particularly for the locally optimised design.

Figure 5 shows the simulated longitudinal phase space coverage of the drive beam bunch [7] for the CG-g

design. In the absence of CSR, the longitudinal bunch profile is virtually unchanged from the start (red) to the end (blue) of the TAL. With CSR included in the tracking simulation, the core of the bunch is significantly distorted (green). Although the higher order chromatic terms in the CG-g design are small, their impact on the off-energy particles in the core of the bunch results in the large horizontal emittance growth observed.

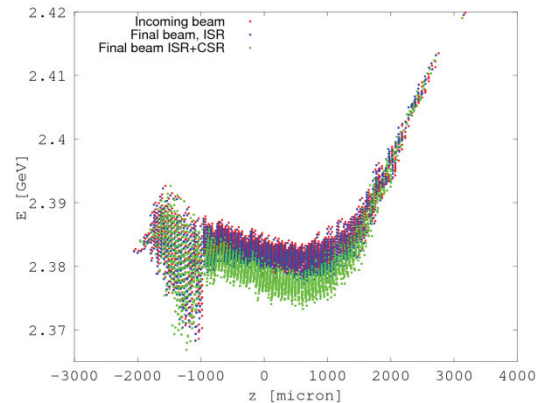


Figure 5: Longitudinal phase space in the TAL with and without CSR.

CONCLUSIONS

The latest design of the final turnaround region for the CLIC drive beam is presented, including the extraction from the long transfer line. Two arc cell designs were investigated; a three-bend achromat and a modified Chasman-Green cell. The CG lattice is the preferred choice for the TAL lattice. A global optimisation of the optics has yielded a design with small chromatic aberrations, but does not allow for a periodic beam through the arcs. The large dispersion in the CG cell makes it prone to CSR. Further studies are required to search for a more suitable arc cell design which is less susceptible to CSR and does not have large chromatic aberrations.

REFERENCES

- [1] The CLIC collaboration, “A Multi-TeV Linear Collider Based on CLIC Technology: CLIC Conceptual Design Report”, (2012), http://project-clic-cdr.web.cern.ch/project-clic-cdr/CDR_Volume1.pdf
- [2] D. Schulte, R. Tomas, “Dynamic Effects in the new CLIC Main Linac”, PAC’09, Vancouver, May 2009, TH6PFP046, p. 3811.
- [3] P. Skowroński et al., “Design of Phase Feed Forward System in CTF3 and Performance of Fast Beam Phase Monitors”, IPAC’13, Shanghai, May 2013, WEOBB203, p. 2097.
- [4] E.T. d’Amico, G. Guignard, “Special Lattice Computation for the CERN Compact Linear Collider”, PRST-AB 4 021002, 2001.
- [5] PLACET, <https://savannah.cern.ch/projects/placet>
- [6] MADX, <http://mad.web.cern.ch/mad/>

- [7] J. Esberg et al., “Effect of CSR Shielding in the Compact Linear Collider”, these proceedings, TUPME003, IPAC2014.